VERSITA

Thermal stability of nanocrystalline iron[*]

RAFAL. J. WROBEL[†]

Institute of Chemical and Environment Engineering, West Pomeranian University of Technology,
Pułaskiego 10, 70-322 Szczecin, Poland

Nanocrystalline iron was obtained by reduction of magnetite doped with structural promoters at 773 K and characterized by various methods i.e. thermal desorption of gases (BET), X-ray diffraction (XRD) and inductively coupled plasma atomic emission spectroscopy (ICP-AES). Crystallite size distribution was determined using a novel method based on a phenomenon unique to nanomaterials, i.e. the dependence of the crystallite phase transition on the size of the crystallites. Thermal treatment of the nanocrystalline iron in a hydrogen atmosphere at 1073 K revealed that it is thermally unstable. The parameters of the log-normal crystallite size distribution were $d_0 = 15.3$ nm, $\sigma = 0.35$ and $d_0 = 23.5$ nm, $\sigma = 0.17$ for iron treated at 773 K and 1073 K, respectively. The corresponding average crystallite sizes determined from the Scherrer formula were 18 nm and 24 nm, respectively. The size distribution of the sintered materials clearly shows that the thermal stability is a function of the size of the crystallites, i.e. the smallest crystals are the least thermally stable. However, no increase in the contribution of crystallites above 35 nm has been observed. Application of this phenomenon combined with the determination of crystallite size distribution enables fine-tuning of the crystallite size distribution.

Keywords: *nanocrystalline iron, Scherrer, XRD, TGA*

1. Introduction

Nowadays, the prefix "*nano*" has become a buzzword, not only in science but also in mass media. This term is commonly associated with the scientific state of the art. Thus, rapid development of nanotechnology and nanoscience can be observed. "*Nano*" can be spotted in the names of conferences and projects, and in newspaper headlines. Usually, hardly anybody is aware that nanotechnology, i.e. the technology of obtaining materials with unique properties due to the nanometric size of the constituents, has been known for more than hundreds of years [1]. This is particularly visible in heterogeneous catalysis, where nanometric size is indispensable for obtaining high specific surface areas [2]. Iron catalyst, i.e. the nanometric iron sponge, which was applied to the synthesis of ammonia by Fritz

Haber in 1909 [3] is an example of such catalyst. In contrast, nanoscience, i.e. the knowledge of the phenomena responsible for the properties of nanomaterials, has started to develop very recently and may still be considered as a scientific domain in the infant stage. Nanoscience requires the exact values of parameters characterizing the nanomaterials in order to develop a theory describing the nanoworld. This task is not trivial and due to the abundance of such parameters there is an urge to devise novel techniques which would enable their acquisition. The particle size distribution of a nanomaterial constituents is one such important parameter, because it affects, among others, the magnetic and catalytic properties of the material [4, 6]. However, only a small number of methods, such as transmission electron microscopy (TEM) and X-ray diffraction (XRD) allow these kinds of measurements. Both TEM and XRD have serious disadvantages and require tedious work [7, 8]. Therefore, many researchers decide to measure only the average crystallite size with the Scherrer method [9, 11], which is relatively easy to perform using XRD. The average

crystallite size can also be indirectly elucidated from the chemisorption of gases [2, 12].

One of the aims of this paper is to present a novel method for the determination of the crystallite size distribution, which is as straightforward as the Scherrer method. It should be pointed out that the nanocrystalline iron used here serves only as a model material and the method can be applied to other nanocrystalline materials as well.

The other goal of the paper is to present the results of the thermal stability investigation of iron nanoparticles. Materials consisting of nanoparticles have high specific surface areas, which is related to the excess of surface energy, and hence these materials are not in a state of thermodynamic equilibrium. As a result, nanocrystalline materials tend to sinter to larger crystallites, which leads to a decrease in their catalytic activity. This feature of the sintering process can be employed to fine-tune the crystallite size distribution. In this paper, it is demonstrated how the sintering process affects the crystallite size distribution.

2.   Experimental

Nanocrystalline iron was produced by a method similar to the method of obtaining iron catalyst for the ammonia synthesis [13]. Iron oxide was mixed with structural promoters (CaO, SiO_2, Al_2O_3) and subsequently melted by resistive heating. The obtained lava was grained, sieved to a fraction of 1.0 - 1.2 mm, and reduced at 773 K in a hydrogen atmosphere. The product of this process is nanocrystalline iron in the form of spongy porous grains. Due to pyrophoric properties it requires passivation for *ex situ* measurements. The passivation was performed by slow oxidation in oxygen-lean atmosphere (99% nitrogen, 1% oxygen) at room temperature. The chemical composition in wt.%, evaluated by inductively coupled plasma atomic emission spectroscopy ICP-AES (JY 238 ULTRACE, JOBIN-YVON) was: Fe 79.8, Al_2O_3 2.9, CaO 3.0, SiO_2 0.3, the oxides of other elements ca. 1.0, oxygen in the form

of iron oxides 13.0. The surface area measured by the Brunauer-Emmett-Teller method (BET) was 11 m^2/g and the porosity coefficient was 0.5. The average crystallite size of iron evaluated by the Scherrer method [9, 11] was 18 nm. In order to obtain the material of a different crystallite size distribution, part of the material was sintered by polythermal treatment in a hydrogen atmosphere by increasing the temperature to 1073 K at a rate of 5 K/min. The material was kept for 3 h under hydrogen flow at 1073 K and then passivated according to the aforementioned procedure. As a result of the sintering process, the average iron crystallite size increased from 18 nm to 24 nm. Further on in this paper, these samples are referred to as iron stable at 773 K and iron stable at 1073 K.

In the next stage, the crystallite size distribution of iron, stable at 773 K and 1073 K, was determined according to the following procedure. The samples were placed in a monolayer in the platinum sample holder of a reactor. It was a homemade reactor that allowed us to perform measurements of mass changes of the samples (TGA - Thermogravimetric Analysis with a resolution of 0.01 mg/g), as well as the analysis of gas composition in the vicinity of the sample. The reactor was made of suitable materials, which enabled its operation in a corrosive gas atmosphere. The temperature of the reactor was increased to 773 K in a hydrogen atmosphere. Polythermal reduction of iron oxides which takes place during this process is monitored thermogravimetrically by measuring the mass loss. A lack of change of the mass of a sample was considered as the end of the reduction process. Subsequently, the temperature of the reactor was set at 673 K and an ammonia-nitrogen mixture was substituted with hydrogen. The ammonia-nitrogen ratio was set to 1:10, in order to slow down the reaction, the rate of which was controlled by the surface adsorption of ammonia. The increase in the mass of the sample due to the nitriding reaction was measured thermogravimetrically. The construction of the thermobalance and the sample holder as well as the applied thermodynamic conditions allow the nitriding reaction to be controlled by

the surface adsorption of ammonia which is vital to the determination of the crystallite size distribution [14, 16]. From the mass increase, it was possible to evaluate the degree of conversion of iron to the product (Fe₄N). The degree of conversion was confirmed independently by XRD phase analysis. A series of samples, varying in the degree of conversion of iron to Fe₄N, was produced according to the aforementioned procedure. The degree of conversion was controlled by freezing the reaction by rapid cooling of the reactor chamber. For *ex situ* XRD measurements, the passivation process was performed for each sample. The final stage involved XRD analysis and measurements of the average crystallite size of the iron phase present in the samples with different degrees of conversion. CoKα radiation was used to perform these measurements with a Philips X'pert X-ray diffraction spectrometer. The average crystallite size of iron was calculated from the (211) reflection.

3. Results and discussion

Nanocrystalline iron produced according to the aforementioned procedure has a porous structure which is relatively stable at elevated temperatures due to the addition of structural promoters [17]. Fig. 1 presents a 2D model of such a structure.

Owing to the nanometric size of the crystallites, the iron nitriding reaction under abovementioned conditions is driven by the dissociative adsorption of ammonia, which occurs on the iron surface. Since the process is limited by the surface reaction, the phase transition of iron to the Fe₄N phase occurs according to the adsorption range model. Fig. 2 illustrates this model.

The phenomenon is thoroughly described elsewhere [14, 16]. During the reaction, the crystallites react to form the product in accordance with their size, i.e. from the smallest to the largest. In the example given above, the reactant and the product are iron and Fe₄N, respectively. Using the broadening of the XRD peak, the average crystallite size of both the reactant and the product can be evaluated from the Scherrer

Structural promoters - Al₂O₃, CaO, SiO₂
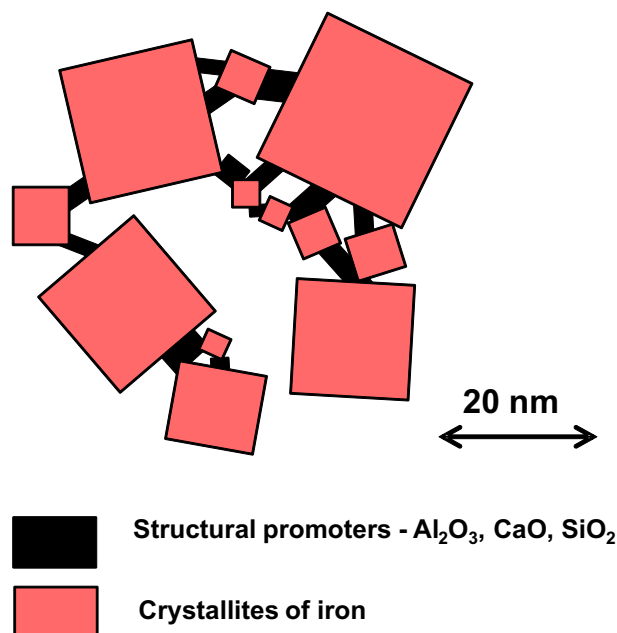
Crystallites of iron

Fig. 1. A schematic 2D representation of nanocrystalline iron with structural promoters.
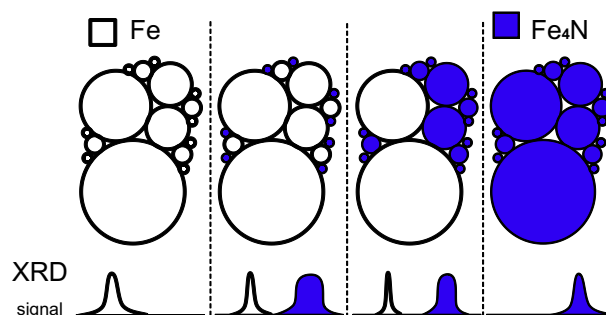

Fig. 2. The concept of the adsorption range model. The influence on the broadening of the XRD peak is presented. The influence on intensity was neglected.

equation (Eq. 1) [9, 11]:

$$\bar{d}_{k(hkl)} = \frac{k \cdot \lambda}{\beta \cdot \cos\theta},\qquad(1)$$

where: $\bar{d}_{k(hkl)}$ – the average crystallite size in the direction perpendicular to the hkl reflection plane; k – a constant close to unity, dependent on the shape of the crystallite; λ - the X-ray wavelength; β - the peak broadening; θ - the XRD peak position.

The reaction can be stopped at any moment. Hence, the dependence of the average crystallite size of the remaining reactant on the conversion degree can be determined. Such dependence can be mathematically deconvoluted, and the crystallite size distribution appearing in the integral form of the Scherrer equation can be determined (Eq. 2) [7]:

$$\beta = \frac{k \cdot \lambda}{\frac{1}{V}\left(\int_0^V d_k(v) \cdot dv\right) \cdot \cos\theta},\qquad (2)$$

where: $d_k(v)$ is the crystallite size as a function of its volume v; V – the total volume of the crystallites.

Fig. 3 presents a TG curve for the nitriding of iron stable at 773 K and a set of corresponding XRD spectra. The samples with varying nitrogen content, denoted with circles on the TG curve, were obtained by freezing the reaction. The *ex situ* XRD phase analysis of these samples reveals two phases, i.e. α-iron (reactant) and γ'-Fe_4N (product).

Fig. 4 presents the plot of α-iron content vs. nitrogen content in the sample. It can be observed that the amount of α-iron phase decays linearly with increasing nitrogen content.

Iron oxides formed during the passivation process cannot be detected due to the amorphous structure of the passivation oxide layer. The broadening of the reflex from iron {211} plane family was used for the average crystallite size measurements with the Scherrer equation (Eq. 1). The dependence of the average crystallite size of iron on the conversion degree was obtained for the samples of iron stable at 773 K and 1073 K, respectively, based on the XRD measurements and is presented in Fig. 5.

The positive slope of the curves (Fig. 5) confirms the validity of the adsorption range model, cf. [14, 16] for details. These references demonstrate that the dependence of the average crystallite size on the conversion degree is directly related to the crystallite size distribution and thus the crystallite size distribution can be determined. However, due to measurement uncertainties, purely mathematical deconvolution may lead to results
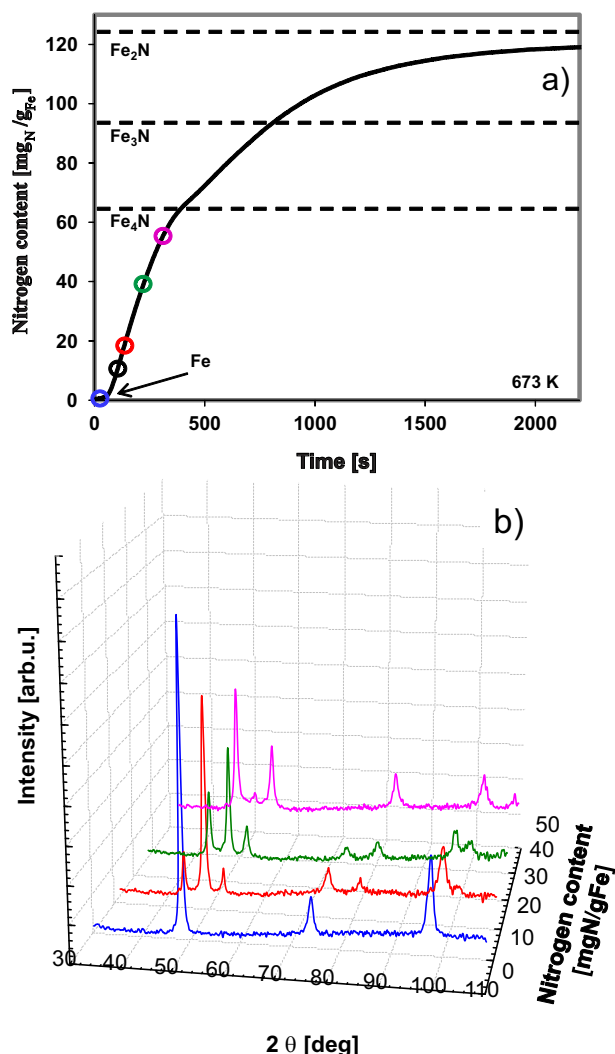
Fig. 3. a) The TG curve of nitriding of iron stable at 773 K conducted at 673 K and under 1 bar ammonia pressure. Dashed lines denote the nitrogen content corresponding to stoichiometric Fe_4N, Fe_3N, Fe_2N, respectively. Circles denote the points on the TG curve corresponding to the nitrogen content of the frozen samples. b) A set of XRD spectra for the iron samples with varying nitrogen content. The nitrogen content corresponds to the circles on the TG curve.

which are not physically meaningful, and artifacts, such as spurious contributions from crystallites with a negative diameter, may appear. To overcome this difficulty, an approach different from the one presented in [14, 16] was applied. Assuming a
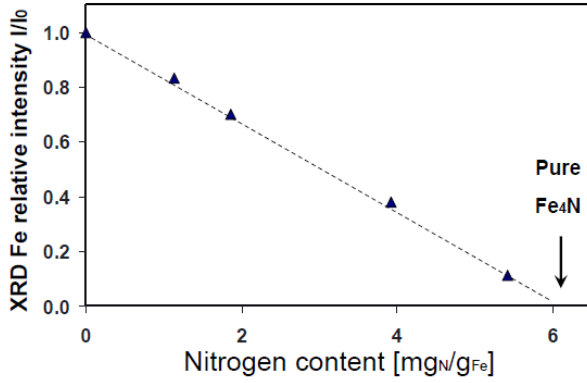
Fig. 4. The iron phase content expressed as a relative intensity vs. the nitrogen content in the sample. The arrow denotes the nitrogen content corresponding to the stoichiometric Fe_4N phase.
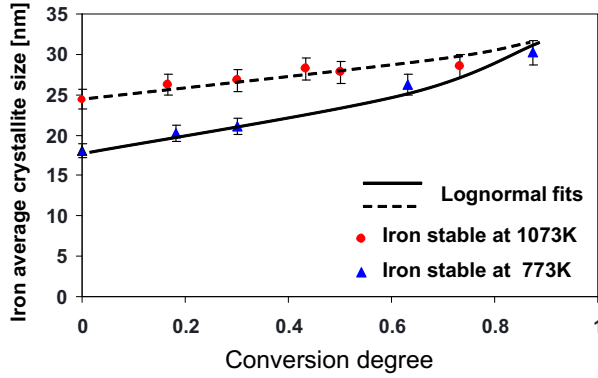

Fig. 5. The dependence of the average crystallite size of iron on the conversion degree for iron stable at 773 K and 1073 K, respectively. Lines denote the dependence obtained from the fitting process with the assumption of a log-normal crystallite size distribution.

log-normal distribution of crystallite sizes, the distribution can be described with Eq. 3. [18]:

$$GSD_{\log norm}(d_k, d_0, \sigma) =$$

$$\frac{1}{d_k\sqrt{2\pi}\sigma} \exp\left(\frac{-\left(\ln d_k - \ln d_0 - \sigma^2\right)^2}{2\sigma^2}\right), \qquad (3)$$

where: GSD – the crystallite size distribution function, d_k- the diameter of the crystallite, d_0 – the diameter of the crystallite corresponding to the maximum of the distribution function, σ – standard deviation.
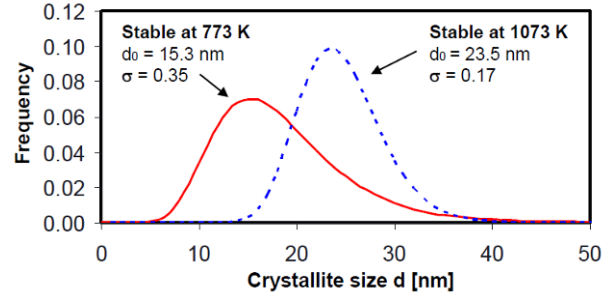

Fig. 6. The crystallite size distribution of nanocrystalline iron stable at 773 K and 1073 K, obtained by the proposed method.

The dependence of the average crystallite size on the conversion degree (Fig. 5) can be precisely calculated for the given crystallite size distribution, assuming the adsorption range model of the process. Accordingly, the parameters of the log-normal distribution were fitted to the experimental data by the application of the least-squares method [19].

The fitting procedure is as follows: the parameters d_0 and σ are assumed arbitrarily (Eq. 3). For the GSD function defined by Eq. 3, the dependence of the average crystallite size on the conversion degree is determined according to Eqs. 4 and 5. From Eq. 4, the conversion degree can be calculated, and from Eq. 5 – it is possible to estimate the average crystallite size for the given conversion degree. The sums of squares of the differences between the model and experimental data are calculated. These sums are minimized in an iterative process in which the parameters d_0 and σ are varied.

$$\alpha = \int_0^D GSD(d_k) \cdot dd_k, \qquad (4)$$

$$\bar{d}_k = \frac{\int_D GSD(d_k) \cdot d_k \cdot dd_k}{1 - \alpha}, \qquad (5)$$

where: α- the conversion degree of iron, $\bar{d}_k$ - the average crystallite size of remaining iron, d_k - crystallite size, D - size of the crystallite which undergoes phase transition at conversion degree α.

The curves presented in Fig. 5 show positive slopes, which is related to the phenomenon of the adsorption range model, mentioned above. The solid and dashed curves were obtained in the fitting process. The parameters of the model used for the fitting process are the same as these used for the estimation of the crystallite size distribution function. Fig. 6 presents two log-normal crystallite size distributions obtained as a result of the fitting process of the parameters d_0 and σ, along with their values.

It can be observed that in the course of sintering, the smallest crystallites disappear and the content of larger crystallites increases. The smaller the crystallite is, the higher the surface energy, and the lower the thermal stability of the crystalite. Therefore, smaller crystallites grow faster than the larger ones. The shape of the distribution after sintering is similar to the Gaussian of Eq. 3, but is significantly narrower (standard deviation σ = 0.17 vs. 0.35). In other words, iron stable at 1073 K is more homogeneous with respect to crystallite sizes, which enables tailoring of the crystallite size distribution through temperature treatment.

Closer inspection of the distribution leads to the conclusion that crystallites smaller than 5 nm are thermally unstable at 773 K, whereas at 1073 K, the smallest stable crystallites measured 15 nm. These crystallites undergo the sintering process to become larger. The content of crystallites larger than 35 nm has not increased in either of cases, which means that such crystallites are thermally stable at 1073 K.

The procedure for the determination of the crystallite size distribution described here is valid not only for the iron – iron nitride system, but can be applied to any nanocrystalline material that undergoes reaction according to the adsorption range model. This model of the process was reported for other reactions, such as carburization [20] and oxidation [21] of nanocrystalline iron. Therefore, the crystallite size distribution method may be applied to a broad range of processes and materials.

4.   Conclusions

Nanocrystalline iron with structural promoters was thermally treated in a hydrogen atmosphere at 773 K and 1073 K, respectively. The application of the phenomenon in which the crystallites undergo phase transition according to their size, combined with TGA and XRD methods, allowed the determination of the crystallite size distributions for both kinds of iron. These distributions clearly show that the sintering process strongly depends on the size of crystallites. Crystallites smaller than 5 nm are not thermally stable above 773 K, whereas above 1073 K this limit is 15 nm. During the sintering process, crystallites ranging from 5 to 15 nm transform into crystallites ranging from 15 to 35 nm. Formation of crystallites larger than 35 nm was not observed. As a result, crystallite size distribution after thermal treatment at 1073 K is significantly narrower (standard deviation σ = 0.17 vs. 0.35) than the one at 773 K. This allows tuning the distribution of nanocrystalline materials through thermal treatment.

Acknowledgments

References

[1] FREUND H.-J., *Surf. Sci.*, 500 (2002) 271.
[2] KIM C. H., THOMPSON L. T., *J. Catal.*, 244 (2006) 248.
[3] MANCHESTER K.L., *Endavour*, 26 (2) (2002) 64.
[4] FISCHER B., WAGNER J., SCHMITT M., HEMPELMANN R., *J. Phys. Condens. Matter*, 17 (2005) 7875.
[5] BARKHUIZEN D., MABASO I., VILJOEN E., WELKER C., CLAEYS M., VAN STEEN E., FLETCHER J. C. Q., *Pure Appl. Chem.*, 78 (2006) 1759.
[6] MEGELSKI S., CALZAFERRI G., *Adv. Funct. Mater.*, 11 (2001) 277.
[7] WARREN B.E., *X-ray diffraction*, Addison-Wesley, Reading, Massachusetts 1969.
[8] LANGFORD J. I., LOUR D., SCARDI P., *J. Appl. Cryst.*, 33 (2000) 964.
[9] KLUG H.P., ALEXANDER L.E., *X-ray diffraction procedures for polycrystalline and amorphous materials*, 2nd ed., J. Wiley, New York-London 1974.

[10] PATTERSON A. L., *Phys. Rev.*, 56 (1939) 978.

[11] LANGFORD J. I., WILSON A. J. C., *J. Appl. Cryst.*, 11 (1978) 102.

[12] SHEN X., GARCES L-J., DING Y., LAUBERNDS K., ZERGER R. P., AINDOW M., NETH E. J., SUIB S. L., *Appl. Catal. A-Gen.*, 335 (2008) 187.

[13] FIGURSKI M. J., ARABCZYK W., LENDZION-BIELUŃ Z., KALEŃCZUK R. J., LENART S., *Appl. Catal. A-Gen.*, 247 (2003) 9.

[14] ARABCZYK W., WRÓBEL R., *Solid State Phenom.*, 94 (2003) 185.

[15] ARABCZYK W., WRÓBEL R., *Solid State Phenom.*, 94 (2003) 235.

[16] WROBEL R., ARABCZYK W., *J. Phys. Chem. A*, 110 (2006) 9219.

[17] SCHLÖGL R., JENNINGS J.R., *Catalytic Ammonia Synthesis*, Plenum Press, New York, 1991, p. 104.

[18] PIELASZEK R., Thesis, University of Warsaw, Physics Department, 2003.

[19] BJORCK A., *Numerical Methods for Least Squares Problems*, Society for Industrial and Applied Mathematics, 1996.

[20] ARABCZYK W., KONICKI W., NARKIEWICZ U., *Solid State Plenom.*, 94 (2003) 177.

[21] LUBKOWSKI K., ARABCZYK W., GRZMIL B., MICHALKIEWICZ B., PATTEK-JANCZYK A., *Appl. Catal. A-Gen.*, 329 (2007) 137.